Research Article | Vol. 25, No. 21 | 16 Oct 2017 | OPTICS EXPRESS 25992

Optics EXPRESS

Propagation analysis of phase-induced amplitude apodization optics based on boundary wave diffraction theory

WEI WANG,[1,2] XIN ZHANG,[1,*] QINGYU MENG,[1,3] AND YUETAO ZHENG[1]

[1]Changchun Institute of Optics, Fine Mechanics and Physics, Chinese Academy of Sciences, No. 3888, Dongnanhu Road, Changchun 130033, China

[2]University of Chinese Academy of Sciences, Beijing 100000, China

[3]Research Center for Space Optical Engineering, Harbin Institute of Technology, Harbin 150000, China

*optlab@ciomp.ac.cn

Abstract: Phase-induced amplitude apodization (PIAA) is a promising technique in high contrast coronagraphs due to the characteristics of high efficiency and small inner working angle. In this letter, we present a new method for calculating the diffraction effects in PIAA coronagraphs based on boundary wave diffraction theory. We propose a numerical propagator in an azimuth boundary integral form, and then delve into its analytical propagator using stationary phase approximation. This propagator has straightforward physical meaning and obvious advantage on calculating efficiency, compared with former methods based on numerical integral or angular spectrum propagation method. Using this propagator, we can make a more direct explanation to the significant impact of pre-apodizer. This propagator can also be used to calculate the aberration propagation properties of PIAA optics. The calculating is also simplified since the decomposing procedure is not needed regardless of the form of the aberration.

OCIS codes: (050.1940) Diffraction; (120.6085) Space instrumentation; (220.2560) Propagating methods.

References and links

1. O. Guyon, “Phase-induced amplitude apodization of telescope pupils for extrasolar terrestrial planet imaging,” Astron. Astrophys. **404**(1), 379–387 (2003).
2. O. Guyon, E. A. Pluzhnik, M. J. Kuchner, B. Collins, and S. T. Ridgway, “Theoretical limits on extra solar terrestrial planet detection with coronagraphs,” Astrophys. J. **167**(1 Suppl.), 81–99 (2006).
3. F. Martinache, O. Guyon, E. A. Pluzhnik, R. Galicher, and S. T. Ridgway, “Exoplanet imaging with a phase-induced amplitude apodization coronagraph.II. Performance,” Astrophys. J. **639**(2), 1129–1137 (2006).
4. R. J. Vanderbei, “Diffraction analysis of two-dimensional pupil mapping for high-contrast imaging,” Astrophys. J. **636**(1), 528–543 (2006).
5. R. Belikov, N. J. Kasdin, and R. J. Vanderbei, “Diffraction-based sensitivity analysis of apodized pupil-mapping systems,” Astrophys. J. **652**(1), 833–844 (2006).
6. E. A. Pluzhnik, O. Guyon, S. T. Ridgway, F. Martinache, R. A. Woodruff, C. Blain, and R. Galicher, “Exoplanet imaging with a phase-induced amplitude apodization coronagraph. III. Diffraction effects and coronagraph design,” Astrophys. J. **644**(2), 1246–1257 (2006).
7. L. Pueyo, S. B. Shaklan, A. Give’on, and J. Krist, “Numerical propagator through PIAA optics,” Proc. SPIE **7440**, 74400E (2009).
8. J. E. Krist, L. Pueyo, and S. B. Shaklan, Proc. “Practical numerical propagation of arbitrary wavefronts through PIAA optics,” Proc. SPIE **7731**, 77314N (2010).
9. G. Otis, J. L. Lachambre, J. W. Y. Lit, and P. Lavigne, “Diffracted waves in the shadow boundary region,” J. Opt. Soc. Am. **67**(4), 551–553 (1977).
10. E. Cady, “Boundary diffraction wave integrals for diffraction modeling of external occulters,” Opt. Express **20**(14), 15196–15208 (2012).
11. L. Pueyo, N. J. Kasdin, and S. Shaklan, “Propagation of aberrations through phase-induced amplitude apodization coronagraph,” J. Opt. Soc. Am. A **28**(2), 189–202 (2011).
12. M. Born and E. Wolf, *Principles of Optics* (Cambridge University, 1999).
13. R. J. Vanderbei and W. A. Traub, “Pupil mapping in two dimensions for high-contrast imaging,” Astrophys. J. **626**(2), 1079–1090 (2005).
14. K. Miyamoto, “Effect of boundary diffraction wave in coronagraph,” J. Opt. Soc. Am. **54**(9), 1105–1108 (1964).

#297310 https://doi.org/10.1364/OE.25.025992
Journal © 2017 Received 2 Jun 2017; revised 1 Sep 2017; accepted 16 Sep 2017; published 11 Oct 2017

Optics EXPRESS

15. T. Suzuki, "Extension of the Theory of the Boundary Diffraction Wave to Systems with Arbitrary Aperture-Transmittance Function," J. Opt. Soc. Am. **61**(4), 439–445 (1971).
16. Y. Z. Umul, "Uniform boundary diffraction wave theory of Rubinowicz," J. Opt. Soc. Am. A **27**(7), 1613–1619 (2010).

1. Introduction

The Phase-induced Amplitude Apodization (PIAA) coronagraph, which was first proposed by Guyon [1], is a very promising technique for high contrast imaging of exo-planets. It employs sets of (at least two) aspherical optical elements to achieve the pupil apodization. Hence, it has good performance offering high contrast, high throughput and smaller inner working angle [2,3]. One important issue for PIAA coronagraph design is the computing of diffraction effects, because the high contrast apodization redistribute light from the edge of the entrance pupil to a more widely area of the exit pupil, which dramatically amplifies the diffraction effects, and notably influences the final contrast performance. However, in the case of PIAA, as Vanderbei pointed out [4], Fresnel diffraction modeling does not work well. Various alternative methods with higher accuracy have been proposed [4–8]. Propagators in [4–6] are based on Huygens wavelet propagation, which has the form of 2-dimensional surface integral or a reduced radial integral using Bessel functions. In [7], Pueyo derived a modification of the angular spectrum propagation algorithm that can be used for PIAA systems. In [8], Krist optimized this method by combining it with S-Huygens method (proposed in [5]) to reduce the number of wavefront components, and the calculating efficiency was proved to be higher.

In this paper, we will derive another propagator of diffraction effects in PIAA optics based on boundary wave diffraction theory. According to boundary wave diffraction theory, the diffraction fields can be described in terms of boundary diffraction waves with the form of 1-dimensional boundary integral, and depending on the situation, the geometrically incident wave [9]. The same method has been successfully used in the design and calculation of external occulter [10]. First, we will approach the specific expression of boundary wave integral in PIAA systems. Then, we will derive an analytical propagator on the basis of the line integral form, using stationary phase approximation, and compare the calculating speed and accuracy with former methods. When pre-apodizer is used, which is a method for mitigating diffraction effects in PIAA systems proposed in [6], we can make a more direct explanation to the effects of pre-apodizer, although an additional term should be added in the propagator. In the last section, we use the analytical propagator for calculating the aberration propagation through PIAA optics. Compared to the decomposing strategy proposed in [5, 11], this propagator is more direct and simplified.

2. Boundary wave diffraction theory in PIAA optics

We start from the basic form of boundary wave diffraction theory [12]. The diffraction field at the exit pupil can be expressed as

$$\begin{cases} U(P) = U_G(P) + U_B(P),\ P\ in\ illuminated\ region \\ U(P) = U_B(P),\ P\ in\ shadow\ region \end{cases}, \tag{1}$$

where $U_G(P)$ is the geometrical propagation wave, and $U_B(P)$ represents the boundary wave. Here the diffraction is assumed to occur on the input surface of L1, and the boundary diffraction theorem is applied on the edge of L1. In a circularly symmetric PIAA system (see Fig. 1), assumed pure geometrical optics, the amplitude profile at the exit pupil can be exactly expressed as the apodization function A, and the electric field distribution is

$$U_G(\tilde{r},\tilde{\theta}) = A(\tilde{r})e^{jkP_0}, \tag{2}$$

where k is the wave number, and P_0 is the constant defined in [13], representing the optical path length for an on-axis ray through the system.

Optics EXPRESS

The boundary wave term in vector form is expressed as [14] which shown in Eq. (3).

$$U_B(\tilde{r},\tilde{\theta}) = \frac{1}{4\pi}\int_\tau \frac{e^{jk\left[S+|n|Z-|n|h(r)+|n|\tilde{h}(\tilde{r})\right]}}{S}\cdot\frac{\vec{p}\times\vec{s}}{1-\vec{p}\cdot\vec{s}}\cdot d\vec{l}. \tag{3}$$

n is the refractive index of the two lenses L1 and L2. n is -1 when the optical elements are both mirrors. $\vec{p}$ represents the unit vector of the geometrically reflective ray of the incident ray. S represents the distance from the point (r_1, θ) on the edge of L1 to the point ($\tilde{r}$, $\tilde{\theta}$) on L2, with $\vec{s}$ as the corresponding unit vector,

$$S = \sqrt{r_1^2+\tilde{r}^2-2r_1\tilde{r}\cos(\theta-\tilde{\theta})+[h(r_1)-\tilde{h}(\tilde{r})]^2},\quad \vec{s} = \frac{1}{S}\begin{pmatrix}\tilde{r}\cos\tilde{\theta}-r_1\cos\theta\\ \tilde{r}\sin\tilde{\theta}-r_1\sin\theta\\ \tilde{h}(\tilde{r})-h(r_1)\end{pmatrix} \tag{4}$$

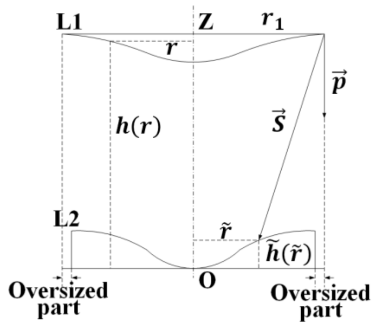

Fig. 1. PIAA system composed by a pair of specially figured lenses. Light incomings from the top. The maximum size of L1 is noted by r_1. L1 is a little oversized in order to mitigate the diffraction effects.

In the case that the two lenses have the same aperture size, that is, $r_{1max} = r_{2max}$, the ray on the edge of L1 is remapped to the exact edge of L2. Hence, the incident ray, the normal vector of L1, and the reflective ray are all along z-axis, and the $\vec{p}$ vector is $(0,0,-1)^T$. When we calculate the output wave at the exact bound of L2, which means $\vec{s}=(0,0,-1)^T$ and $1-\vec{p}\cdot\vec{s}=0$, and the integral is infinite. However, in actual PIAA cases, L1 is slightly oversized (usually several percent) compared with L2, in order to mitigate the diffraction effects [5, 6, 11]. The infinite situation will be avoided. The oversized part of L1 is the constant-curvature extension of the original part. Considering that the curvature at the edge of L1 is usually very weak when the mitigating method of [10] has been used, we make an approximation that $\vec{p}$ is still $(0,0,-1)^T$ in the oversized case. The differential element $d\vec{l}$ can be expressed as

$$d\vec{l} = r_1 d\theta\cdot(\sin\theta,\quad -\cos\theta,\quad 0)^T. \tag{5}$$

Using expression (4) and (5), we transfer (3) to the scalar form,

$$U_B\left(\tilde{r},\tilde{\theta}\right) = \frac{1}{4\pi}e^{jk|n|\left[Z-h(r_1)+\tilde{h}(\tilde{r})\right]}\int_0^{2\pi}\frac{e^{jkS}}{S}\cdot\frac{r_1\left[\tilde{r}\cos\left(\theta-\tilde{\theta}\right)-r_1\right]}{S+h\left(r_1\right)-\tilde{h}\left(\tilde{r}\right)}d\theta, \tag{6}$$

Substitute (2) and (6) into (1), then we can obtain the diffraction field at the exit pupil within the maximum aperture of L2,

Optics EXPRESS

$$U\left(\tilde{r},\tilde{\theta}\right)=A\left(\tilde{r}\right)+\frac{1}{4\pi}e^{jk\left\{\left|n\right|\left[Z-h\left(r_1\right)+\tilde{h}\left(\tilde{r}\right)\right]-P_0\right\}}\int_0^{2\pi}\frac{e^{jkS}}{S}\cdot\frac{r_1\left[\tilde{r}\cos\left(\theta-\tilde{\theta}\right)-r_1\right]}{S+h\left(r_1\right)-\tilde{h}\left(\tilde{r}\right)}d\theta. \quad (7)$$

Here we shift the phase by e^{-jkP_0} for simplification. Equation (7) is the boundary wave expression of the output field through PIAA optics. It is composed by a geometrical apodization function and an azimuthal integral along the boundary of L1. The reduction from 2D integral to 1D integral is very important to the calculating efficiency, as proposed in [5]. While the difference from [4, 5] is that we do not use Bessel function in the integral and the only oscillating term in the integrand is e^{jkS}.

3. Stationary phase approximation and the analytical expression

Since the boundary wave integral has the form of exponential oscillating, we can approach the integral expression by stationary phase approximation [12]. By the stationary phase approximation, 1-dimensional integral with the following form can be calculated by

$$I\left(k\right)=\int_{-\infty}^{+\infty}g\left(x\right)e^{jkf\left(x\right)}dx=\operatorname{sgn}\left[f''\left(x_0\right)\right]\sqrt{\frac{2\pi}{kf''\left(x_0\right)}}g\left(x_0\right)e^{jkf\left(x_0\right)}e^{j\frac{\pi}{4}}, \quad (8)$$

where x_0 are the critical points which satisfy $f'(x_0)=0$. Here we should make the assumption that k is very large and $g(x)$ changes slowly. For the boundary wave diffraction Eq. (6),

$$\begin{aligned}&\int_0^{2\pi}\frac{e^{jkS}}{S}\cdot\frac{r_1[\tilde{r}\cos(\theta-\tilde{\theta})-r_1]}{S+h(r_1)-\tilde{h}(\tilde{r})}d\theta\\&=\lim_{N\to\infty}\frac{1}{2N}\int_{-2N\pi}^{2N\pi}\frac{e^{jkS}}{S}\cdot\frac{r_1[\tilde{r}\cos(\theta-\tilde{\theta})-r_1]}{S+h(r_1)-\tilde{h}(\tilde{r})}d\theta\\&\approx\frac{1}{2N}\int_{-\infty}^{+\infty}e^{jkf(\theta)}g(\theta)d\theta,\end{aligned} \quad (9)$$

where

$$f\left(\theta\right)=S\left(\theta\right)=\sqrt{r_1^2+\tilde{r}^2-2r_1\tilde{r}\cos\left(\theta-\tilde{\theta}\right)+\left[h\left(r_1\right)-\tilde{h}\left(\tilde{r}\right)\right]^2}, \quad (10)$$

$$g(\theta)=\frac{r_1[\tilde{r}\cos(\theta-\tilde{\theta})-r_1]}{S[S+h(r_1)-\tilde{h}(\tilde{r})]}, \quad (11)$$

Hence, the critical points are

$$\begin{cases}\sin(\theta-\tilde{\theta})=0\\ \theta=\tilde{\theta}+m\pi, m=-2N,-2N+1,\ldots\ldots,2N-1\end{cases}. \quad (12)$$

When m is even,

$$\begin{cases}\cos(\theta-\tilde{\theta})\\ \dfrac{\partial^2 f}{\partial\theta^2}=\dfrac{r_1\tilde{r}}{S_1}, S_1=\sqrt{(r_1-\tilde{r})^2+[h(r_1)-\tilde{h}(\tilde{r})]^2}\end{cases} \quad (13)$$

For any stationary point, we obtain

$$I_1=\sqrt{\frac{2\pi S_1}{kr_1\tilde{r}}}\cdot\frac{r_1\tilde{r}-r_1^2}{S_1\left[S_1+h\left(r_1\right)-\tilde{h}\left(\tilde{r}\right)\right]}e^{jkS_1}e^{j\frac{\pi}{4}}, \quad (14)$$

Optics EXPRESS

Also we can obtain the result when m is odd,

$$\begin{aligned} I_{-1} &= \sqrt{\frac{-2\pi S_{-1}}{kr_1\tilde{r}}} \cdot \frac{r_1\tilde{r}+r_1^2}{S_{-1}\left[S_{-1}+h(r_1)-\tilde{h}(\tilde{r})\right]} e^{jkS_{-1}} e^{j\frac{\pi}{4}}, \\ \mathrm{S}_{-1} &= \sqrt{(r_1+\tilde{r})^2+\left[h(r_1)-\tilde{h}(\tilde{r})\right]^2} \end{aligned} \tag{15}$$

Hence,

$$\int_0^{2\pi} \frac{e^{jkS}}{S} \cdot \frac{r_1[\tilde{r}\cos(\theta-\tilde{\theta})-r_1]}{S+h(r_1)-\tilde{h}(\tilde{r})} d\theta = (2NI_1+2NI_{-1})/2N = I_1+I_{-1}. \tag{16}$$

Substitute Eq. (16) into (7), we obtain an analytical expression of the diffraction field,

$$U(\tilde{r},\tilde{\theta}) = A(\tilde{r}) + (1/4\pi) e^{jk\left\{|n|\left[Z-h(r_1)+\tilde{h}(\tilde{r})\right]-P_0\right\}} \cdot (I_1+I_{-1}). \tag{17}$$

Equation (17) can be used as the analytical propagator of diffraction effects in PIAA optics. Compared to former numerical propagators, the physical meaning of Eq. (17) is much more straightforward: the propagator can be divided into the geometrical part and the diffractive part. The diffractive part is determined by the boundary wave of two edge points. One have the same azimuth angle as the calculated point, and another is the opposite point.

Furthermore, from the view of calculation efficiency, using Eq. (17) will be even faster since all of the calculation is done in one analytical expression. The improvement on propagator's calculating efficiency is significant to PIAA systems, due to the need of active wavefront control and iterative system performance modeling [8].

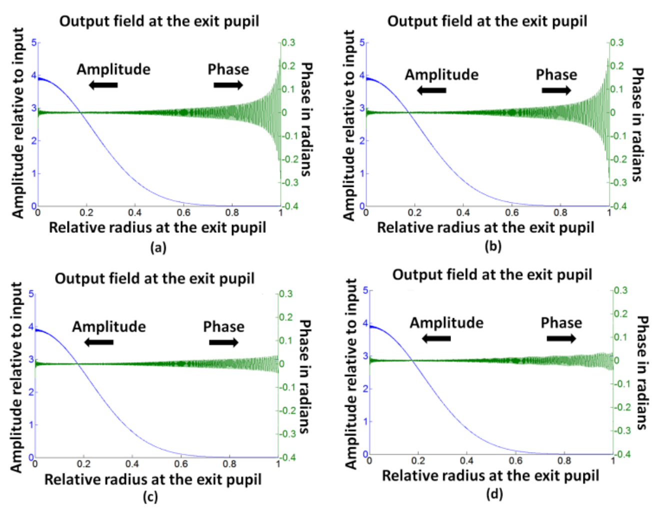

Fig. 2. The output fields calculated by four different methods: boundary wave integral *(a)*, stationary phase approximation of boundary wave *(b)*, S-Huygens approximation of 2D integral *(c),* and hybrid PASP method *(d)* proposed by Krist [8]. The radius of the second mirror is 50mm, and the first mirror is 2% oversized. The mirror separation is 500mm. The incoming light wavelength is 800nm.

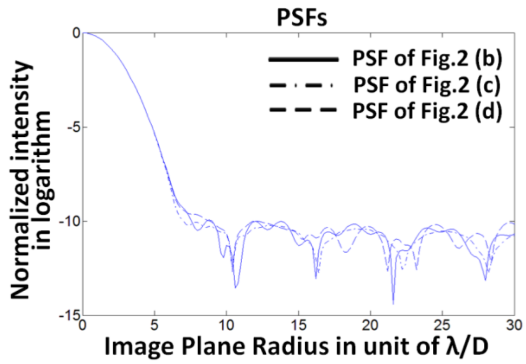

Fig. 3. PSFs at the focus of PIAA system, corresponding to the three output fields *(b)*, *(c)*, and *(d)* obtained above. The PSFs were computed by 10,000 points discretization.

To prove the efficiency and accuracy of Eq. (17), we take the case of a reflective PIAA system with post apodization but without pre-apodizer as an example. Cases with pre-apodizer will be dealt with in the next section since it is a little more complicated. A typical Gaussian amplitude profile approximately matching a high contrast profile

$$A(\tilde{r}) = a \cdot e^{-10(\tilde{r}/R)^2} \tag{18}$$

is employed, where a is a normalization parameter. For mitigating the diffraction effects, as Pluzhnik proposed [6], we oversize the first mirror by 2% and employ a post-apodizer, limiting the minimum value of the apodization to 0.1. Figure 2 shows the diffraction field at the exit pupil, respectively calculated using the boundary wave diffraction integral expression (7), the analytical expression by stationary phase approximation (17), the S-Huygens approximation, and the hybrid PASP method. From the results (a) and (b), we can conclude that the stationary phase approximation shows very high accuracy, since the maximum difference is less than 1.7% in amplitude and 0.015 rad in phase. Results (c) and (d) show very good accordance, 0.5% difference in amplitude and 0.005 rad difference in phase. It is easy to understand since the edge diffraction effects in hybrid PASP method is actually calculated by S-Huygens method. The relative difference in amplitude between (b) and (c) (d) is less than 2% at most positions, while the maximum difference is no more than 20% (occurred at the very near edge). The phase discrepancy near the edge is about 0.24 rad. This discrepancy can be distinguished in the figure but actually very small, since the electric field near the edge is very weak. This is mainly owing to the divergent tendency of boundary wave diffraction theory near the edge of the illumination area. Although the first mirror is oversized and the infinity value is avoided, the discrepancy of boundary wave theory and Kirchoff theory has an increasing trend. But anyhow it does not change the imaging contrast obviously (see Fig. 3 for the corresponding point spread functions, all results can be reduced to below 10^{-10}), because the contribution of the edge to the final PSF is very weak. Hence, these results verify that the boundary integral and the stationary phase approximation have sufficient precision for diffraction analysis in PIAA optics.

On the other hand, from the view of efficiency, we compared the four methods on a normal PC by calculating 10000 points at the output surface. The two 1D integration methods, S-Huygens approximation and boundary wave integration, were executed based on adaptive Gauss-Kronrod (15$^{\text{th}}$ and 7$^{\text{th}}$ order formulas) numerical methods, due to its high efficiency on the quadrature of oscillating integrands. The relative error upper-band was set to 10^{-4}. In the calculation by hybrid PASP algorithm, the highest sampling frequency was 100. The relative errors at most points were below 10^{-4} compared to the case that the highest sampling rate is doubled. In the premise of same calculation accuracy, we can now compare

Optics EXPRESS

the efficiency. The analytical propagator Eq. (17) finished the calculation within one second, while the hybrid PASP method cost about 2~3 minutes (did not include the time for the edge diffraction term computed by S-Huygens method since this procedure is needed only once and can be done previously), and the S-Huygens method cost over 40 minutes. The boundary wave integration cost about 10 minutes, also faster than S-Huygens method, although both of them have a 1D integration form. This difference is mainly due to the Bessel function term in S-Huygens integration making the integrand more oscillating. This comparison demonstrates that the stationary phase approximation of boundary wave is a very efficient method for PIAA propagation.

4. Propagation of PIAA with pre-apodizers

The concept of pre-apodizer in PIAA systems was first proposed by Pluzhnik [6] for mitigating the diffraction effects. The function of pre-apodizer can be quantitatively explained by boundary wave diffraction theory, but first we should do a little modification to Eq. (17) when a pre-apodizer is used.

According to the extension theory of boundary wave diffraction raised by Suzuki [15], when the boundary wave diffraction theory is applied to the aperture with non-uniform transmittance distribution, every point where the gradient of the transmittance is not zero will be the origin of a secondary wave. Here, for simplicity, we will not derive the theorem but directly use the conclusion of Suzuki (Eq. (13) and (14) in [15]). Thus, the boundary wave term at the exit pupil within L2 can be expressed as

$$U_B(\tilde{r},\tilde{\theta}) = \frac{1}{4\pi}\int_\tau T(r_1)\overrightarrow{W}\cdot d\vec{l} - \frac{1}{4\pi}\iint\left(\nabla T(r,\theta)\times\overrightarrow{W}\right)\cdot\vec{n}dS. \tag{19}$$

where T describes the transmittance distribution on the aperture, $\overrightarrow{W}$ is the vector form integrand in Eq. (3), S is the input aperture surface and $\vec{n}$ is the normal vector of S. The first term in Eq. (19) is same as the normal condition while only multiplied by the transmittance function on the edge of L1. Obviously, for mitigating diffraction effects, when we choose the transmittance as zero on the edge of L1, or a continuous edge in another word, the first diffraction term is reduced to zero. As to the second term, the transmittance within the working part of L1 is uniform and the apodization is only employed in the oversized part so that it does not influence the PIAA. Thus, the integration in the second term is only within the oversized surface. Considering that an exponential oscillating term is contained in $\overrightarrow{W}$, we can also use 2D stationary phase approximation to evaluate the integration. From the geometrical theorem of PIAA optics [13], it is easy to understand that for a given point at the exit pupil, the only stationary phase point is the geometrically corresponding point at the entrance pupil, and hence there will not be any stationary phase point in the oversized part. So the contribution of the second term is actually so small that can be neglected in the propagation. Hence, the PIAA system will show exactly geometrical propagation characteristics when a proper pre-apodizer used.

From these analyses, we can conclude three requirements that a pre-apodizer function should satisfy:

1. The transmittance at the outer edge of L1 should to be zero, so as to make the first term zero in Eq. (19), or realize a continuous edge in another word.
2. The transmittance and its first-order derivative at the edge of working part on L1 should be continuous. This requirement comes from the condition for Stokes theorem holding [15], which is the origin of Eq. (19).

Optics EXPRESS

3. The first-order derivative at the outer edge of L1 should also be equals to zero. This is a necessary condition to make the second term in Eq. (19) convergent, since the value of $\vec{W}$ is infinity at the outer edge.

Inversely, we can also know that any pre-apodizer function meeting the three requirements above will make the PIAA system "diffraction-free", for example, the widely used cosine-tapered function. The mitigating effects have been demonstrated numerically by Pluzhnik [6]. We also did the same demonstration with the same PIAA system with Chapter 3 and a cosine-tapered pre-apodizer. The output field in Fig. 4(a), calculated by S-Huygens method, shows smooth profile without any high-frequency oscillations or Arago spot. The PSF at the first focus also shows good accordance with the geometrical results. In addition, we calculate the second term in Eq. (19) and its contribution to final PSF numerically. The results are showed in Fig. 5. The output field contribution of this term is usually at the level of 10^{-6}, and increases rapidly at the very near edge. The relative proportion is nearly 50% at the bound, but similar as the results in Section 3, its contribution to final imaging contrast is very small (See Fig. 5(b)). The highest relative change is at the level of 10^{-3} except at several "valley" points. So this proves additionally that the diffraction term can be neglected when a proper pre-apodizer is used, and the PIAA system will show exactly geometrical propagation properties.

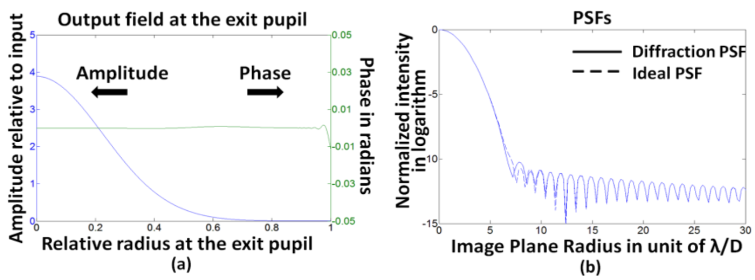

Fig. 4. Output fields and PSFs of a "diffraction-free" PIAA system with cosine-tapered pre-apodizer.

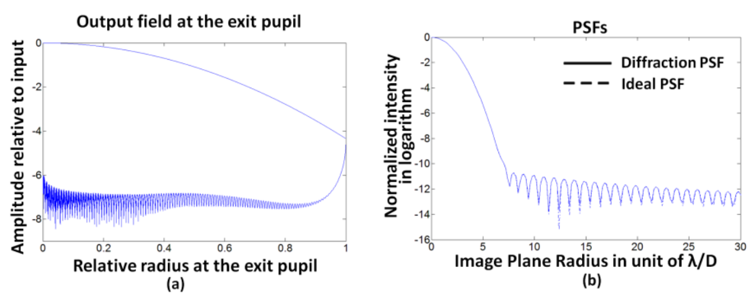

Fig. 5. (a) Output field of the second term of Eq. (19) and (b) its contribution to final PSF. In (a), the upper line is the profile of the apodization function, representing the geometrical propagation properties of PIAA systems. The lower line is the contribution of the second term of Eq. (19), representing the diffraction part properties.

5. Aberration propagation through PIAA optics

By use of Eq. (17), calculating the propagation of aberrations through PIAA optics is also more simplified. Suppose the incoming light has both amplitude errors and phase errors, the input field is written as

$$E(r,\theta) = E_A(r,\theta)e^{jkE_p(r,\theta)}. \tag{20}$$

The only difference from the derivation of (19) is the change of $g(\theta)$,

Optics EXPRESS

$$g(\theta) = \frac{r_1[\tilde{r}\cos(\theta-\tilde{\theta})-r_1]}{S[S+h(r_1)-\tilde{h}(\tilde{r})]}\cdot E(r_1,\theta), \tag{21}$$

Similarly, the final output field can be written as

$$U(\tilde{r},\tilde{\theta}) = A(\tilde{r})E(\tilde{R}(r),\tilde{\theta}) + \frac{1}{4\pi}e^{jk\{|n|[Z-h(r_1)+\tilde{h}(\tilde{r})]-P\}}\cdot[I_1E(r_1,\tilde{\theta})+I_{-1}E(r_1,\tilde{\theta}+\pi)] \tag{22}$$

Equation (22) can be used as an analytical aberration propagator for PIAA systems. It should be noted here that the input field is non-uniform when wavefront errors exist, and we should employ Eq. (19) rather than Eq. (17) rigorously. However, in actual cases, the wavefront errors are at the level of 1/100 λ, and the derivatives of the errors are even smaller. Hence we neglect this factor and still use Eq. (17) for calculation, as long as the aberration scale is small and the frequency is not high. Numerical results compared to the former two methods also verified this point. We take a simple case as an example, assuming a 1/100 λ spherical aberration on the same PIAA optics as Section 3. Figure 6 shows the output field distribution along the axial direction calculated by Eq. (22) (a), S-Huygens method (b), and hybrid PASP method (c) respectively, as well as the imaging contrast (also along the axial direction) of the three fields (d). The corresponding 2D images are shown in Fig. 7. The appearance is similar to the condition with no aberrations. The three results show good accordance at most points but differ at the near edge. From the 2D images in Fig. 7, the discrepancy at the very near can be seen more directly. While this difference still does not change the imaging contrast obviously. That means the propagator based on boundary wave diffraction is also suitable to the aberration propagation in PIAA optics. Compared to former methods, this analytical propagator has obvious improvement on simplification. The former methods for calculating the aberration propagation are based on decomposing the aberration into particular form, Zernike polynomials in [5] and harmonic ripples in [8, 11].While using Eq. (22), the output field can be directly obtained without the procedure of decomposing, no matter what form the aberration is.

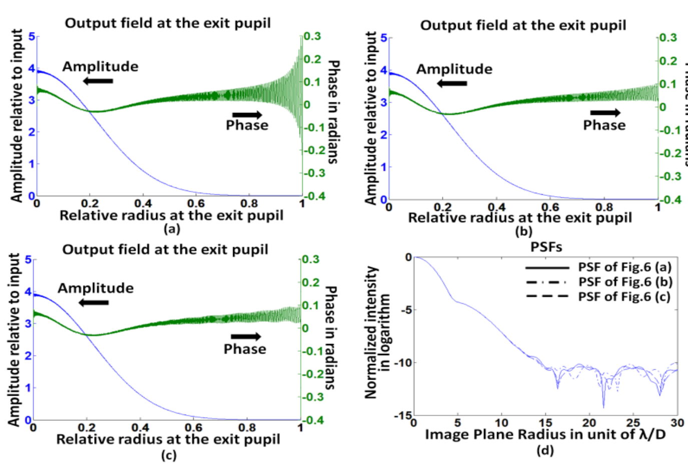

Fig. 6. The output fields calculated by three different methods: stationary phase approximation of boundary wave*(a)*, S-Huygens approximation of 2D integral*(b),* and hybrid PASP method *(c)* proposed by Krist [8].The relative difference in amplitude between (b) and (c) (d) is less than 1.5% at most positions, while the maximum difference is no more than 21% (occurred at the very near edge). The discrepancy in the phase near the edge is about 0.25 rad. However, all of the corresponding PSFs show good accordance while the main differences occur at the “valley” points.

Optics EXPRESS

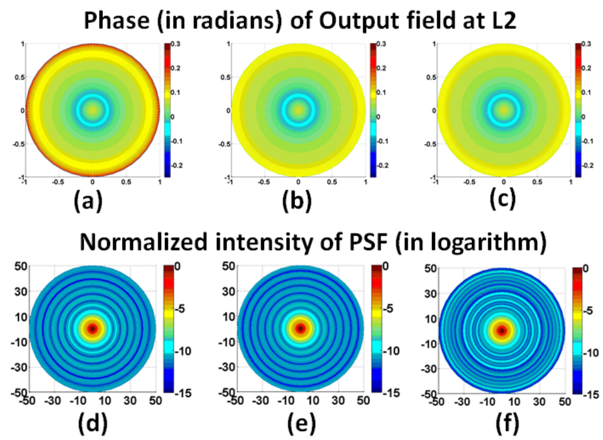

Fig. 7. *Up*: The phase of output fields calculated by three different methods, corresponding to the results in Fig. 6 *(a) ~(c)*. From the 2D images, the discrepancy at the very near can be seen directly. *Bottom*: The PSFs at the focal plane of the corresponding electric fields *(a) ~(c)*, stationary phase approximation *(d)*, S-Huygens approximation *(e),* and hybrid PASP method *(f)* respectively.

6. Summary

In summary, for the first time, we proposed an analytical propagator for calculating the diffraction effects and aberration propagation in PIAA optics based on boundary wave diffraction theory. The expression has straightforward physical meaning, composed of a geometrical part and a boundary wave part. We compared this propagator with former amateur methods, and the results verify the effectiveness and accuracy. According to this propagator, we also present an analytical expression without any decomposing procedure for calculating the aberration propagation through PIAA systems.

The analytical propagator presents much improvement on simplification and efficiency than former numerical propagators, and hence, is very meaningful to future PIAA system design and error budgeting. It can be used in system design and evaluation to predict not only the design performance but also the realistic system with errors. Lots of time can be saved in the iteration process of design and analysis. Furthermore, the most pressing need for an efficient propagator is for wavefront control [8]. Setting up the response matrix needs tremendous times of propagation calculation (determined on the number of DM actuators and sensing wavelength), and the analytical propagator will also save much time on this procedure.

In next step, we will focus on the application of this analytical propagator on the systems with complicated apertures. The propagator in this paper is not suitable to this case since the integrand is infinite at the exact edge but there is no chance of oversizing for spiders of other obscures. In this case, a recent theory called uniform theory of boundary wave diffraction will be considered [16], and the integration should be done along the axial direction, which may also make the propagator more complicated.

Funding

National Natural Science Foundation of China (NSFC) (61705220).